

■ Scientific Justification

All cosmological galaxy formation models have a common feature: they need star formation feedback to reproduce the characteristics of galaxies, drive galactic outflows, and pollute the intergalactic medium with metals (Somerville & Davé 2015). Despite this consensus, there are limitations to our understanding of the physics of galaxy growth. In simulations, the strength of stellar feedback must be “tuned” to match galaxy scaling relations (e.g. mass functions; Oppenheimer & Davé 2008; Dutton et al. 2012; Hopkins et al. 2014; Vogelsberger et al. 2014; Wang et al. 2015; Schaye et al. 2015). The sub-grid physics is still debated.

Observations of galactic outflows can offer discerning tests for feedback models. Simulations using different feedback produce very different outflows. For example, cosmic ray driven winds are thought to produce volume filling slow outflows of cold gas (e.g. Wiener et al. 2017), whereas supernova driven winds should exhibit more clumps (Chevalier & Clegg 1985). Therefore, observations aim to distinguish feedback models by measuring scaling relations between outflow properties (mass-loss rate, \dot{M}_{out} , and outflow velocity, v_{out}) and galaxy properties (e.g. stellar mass, M_* , star-formation rate, SFR, and SFR surface density, Σ_{SFR}). So far, there is no consensus (e.g. Rupke et al. 2005; Weiner et al. 2009; Kornei et al. 2012; Martin et al. 2012; Rubin et al. 2014; Heckman & Borthakur 2016; Chisholm et al. 2016). For example, measurements made on much of the same low-redshift HST/COS data, but using different methods, find substantial differences in the slope and normalization of the \dot{M}_{out} - M_* correlation (Heckman et al. 2015; Chisholm et al. 2017). Consequently, observations struggle to inform theoretical research.

The challenge in measurements of outflows lies in a number of uncertain assumptions, which yield large systematic errors. Therefore, we propose to determine how to interpret outflow measurements from galaxies, as they are frequently made using UV spectra from COS. By observing hydrodynamical simulations as if they were real galaxies, we will use different methods to measure v_{out} and \dot{M}_{out} from mock spectra. Comparing the results to the properties directly measured from the simulations will demonstrate how best to measure outflows. Critically, we propose a first-of-its kind joint modeling and analysis of Ly α and interstellar metal lines. Combined, these diagnostics will provide powerful constraints on gas with a range of physical conditions.

1. Sources of Uncertainty in Outflow Measurements

To understand why observations struggle to provide accurate outflow measurements, it is important to consider how they are estimated. **Figure 1** (right) shows an example of an absorption line profile that could be used to measure an outflow (in this case, a doublet). The mass loss rate would be estimated from the equation:

$$\dot{M}_{out} = \Omega \mu m_p n(r) v(r) r^2 \approx \Omega \mu m_p N v_{out} R_w. \quad (1)$$

Here, Ω represents the solid angle subtended by the outflow, μm_p is the mean mass per particle, and $n(r)$ and $v(r)$ are density and velocity as a function of radius, r . With some assumptions, \dot{M}_{out} can be cast in terms of R_w , the characteristic radius of the wind, as well as the column density, (N) and the outflow velocity (v_{out}), both measured from spectra.

To first order, the uncertainties are easy to understand: Ω and R_w must be assumed since they are not easily constrained by data. However, there are further difficulties. These include, but are not limited to: **(1)** large, uncertain metallicity and ionization corrections are required to infer total gas column density from metal tracer ions (e.g. Martin et al. 2012); **(2)** Resonant scattering in metals “fills” in the absorption (illustrated in **Figure 1**), thereby biasing measurements of column densities, covering fractions, and outflow velocities (Prochaska et al. 2011; Scarlata & Panagia 2015); **(3)** Geometric effects, illustrated in **Figure 2**, produce a variety of line profiles when the same galaxy is viewed with different orientations; **(4)** Difficulties interpreting Ly α , where these issues are amplified due to substantial resonant scattering. Although the emergent spectrum depends on the properties of outflows (Kunth et al. 1998; Wofford et al. 2013; Verhamme et al. 2015; Henry et al. 2015; Rivera-Thorsen et al. 2015), we do not understand how to obtain accurate constraints from Ly α . *Overall, these challenges imply that outflow measurements suffer from large uncertainties.*

2. Observations of Hydrodynamical Simulations

We propose to address the difficult interpretation of outflow measurements by creating spectra from radiation-hydrodynamical (RHD) simulations. By analyzing these spectra as if they were real observations, and comparing to the known v_{out} and \dot{M}_{out} from the simulations, we will derive a set of observational best-practices.

The details of our simulations are as follows: **First**, we are using galaxies from the SPHINX cosmological simulation (Rosdahl et al. 2018). The simulation includes state-of-the-art sub-grid models for star formation and supernova feedback, which are calibrated to match the UV luminosity function at high redshift as well as the observed stellar mass to halo mass relation. Reaching a maximum physical resolution better than 10 pc in the ISM, the simulation probes 2000 (100) resolved galaxies with stellar mass $> 10^4 M_\odot$ ($10^7 M_\odot$). In addition, this mass range is extended to a few times $10^{11} M_\odot$, using a set of eleven additional cosmological zoom simulations with the same physics as SPHINX (Mitchell et al. 2018). This combination of high-resolution and RHD produces galaxies with a detailed ISM and a realistic distribution of HII regions, critical for shaping the line profiles in spectra of galaxies. **Next**, we post-process the simulated galaxies with photoionization models, in order to obtain the relative abundances of different ionic species in each cell. **Then**, most importantly, Monte Carlo radiation transport is carried out using the public code, RASCAS (Michel-Dansac et al. 2019). This modeling accounts for the scattering that shapes both metal lines (see **Figure 1**), as well as Ly α . In this regard, our proposed study is the first-of-its kind. In fact, we have already produced spectral profiles in both Ly α and metals; examples are highlighted in **Figure 3**. **Finally**, we will produce a library of synthetic spectra from the simulated galaxies, extracted through different sight lines, and with different evolutionary states. As we describe in the Analysis Plan, we will also model the instrumental effects of COS, including signal-to-noise, spectroscopic apertures, and spectral resolution.

The combined analysis of Ly α and metal lines in our simulated spectra mark an essential step forward. These features represent the *complete* set of outflow-sensitive diagnostics in the UV. Importantly, the Ly α line wings are sensitive to low density, high-velocity gas that is often missed in metal absorption lines (Henry et al. 2015). Yet metal lines may prove

better for measuring the outflow velocity for the bulk of the densest gas, since the velocity structure near the core of the Ly α lines is thought to depend primarily on N_{HI} (Verhamme et al. 2015; Henry et al. 2015, Orlitová et al. 2018). Therefore, for understanding outflows, the combination of Ly α and metal lines is more powerful than either diagnostic alone.

3. What is the best way to measure outflows?

We propose to use our model spectra to test different methodologies for measuring \dot{M}_{out} and v_{out} , comparing mock observations to the properties directly measured from the simulations¹. Critically, in making these tests, we will vary spectroscopic apertures, resolution, and signal-to-noise, in order to model observations made with HST/COS.

Metal Lines: For measuring outflow properties using metal lines, we will test two different approaches. First, we will use the conventional method, directly evaluating the simple analytical model in Equation 1 (right hand side). We will measure outflow velocities and column densities from absorption lines, and make best guesses for the metallicity, ionization state, characteristic wind radius (R_w), and Ω of the outflow (e.g. Martin et al. 2012; Heckman et al. 2015). As is typically done in these analyses, we will ignore the scattered emission filling that is known to bias column densities and outflow velocities. Alternatively, we will consider more sophisticated analyses, fitting idealized models, like those in **Figures 1** and **2** (e.g. Scarlata & Panagia 2015; Zhu et al. 2015; Chisholm et al. 2017; Carr et al. 2018). In addition to accounting for the scattered infilling, a key advantage of this method is that we can fit for Ω and R_w , as well as the radial density and velocity profiles (e.g. $n(r) \propto r^\alpha$, with α allowed to vary). By comparing these mock observations with the simulations, we will determine the efficacy of each observational method, and quantify any systematic differences between our measurements and the simulated outflows.

Ly α : The line profiles of Ly α , combined with metal lines, may yield more robust outflow measurements. First, the Ly α line profile can measure the total column of H I gas, mitigating the need to infer it from tracer ions with enormous corrections. Additionally, Ly α line wings probe low density, high velocity gas that is missed in the metal lines (Henry et al. 2015). Therefore, we will investigate how Ly α can be combined with metals to measure outflows in our mock spectra. Using the fits to the metal line profiles described above, we will identify the family of idealized models that can reasonably reproduce the mock data. Then, we will use RASCAS to model the Ly α line profiles from these idealized distributions of gas. In this way, we will determine if Ly α observations can narrow the range of allowed models, providing more stringent constraints on outflow properties.

4. Significance of Proposed Work

This investigation will make substantial improvements on our ability to constrain outflow properties from observations. By assessing the variety of techniques and data quality currently used, we will improve our interpretation of outflow measurements. In turn, these analyses will lead to more reliable constraints for galaxy formation simulations.

¹From the simulations, we will calculate mass-weighted outflow velocities, and determine \dot{M}_{out} for gas exceeding a range of threshold velocities at a few different radii (as in Muratov et al. 2015).

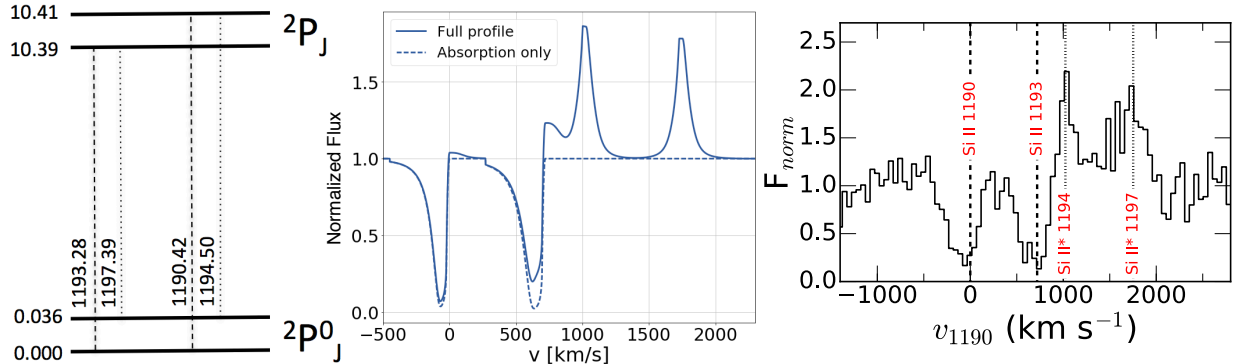


Figure 1: Left— An energy level diagram is shown for the Si II $\lambda\lambda 1190, 1193$ doublet, which is one of the many lines detected in COS UV spectra. Absorption out of the ground state is illustrated by the dashed lines. The excited electron can return to the ground state through either the same dashed lines, filling in the absorption, or through the dotted lines, creating the fluorescent emission lines at $\lambda\lambda 1194, 1197$ Å. The relative contributions from the “infilling” emission and the fluorescent Si II* emission are set by atomic physics. **Center**— Analytic models of the Si II $\lambda\lambda 1190, 1193$ and Si II* $\lambda\lambda 1194, 1197$ Å lines, adapted from Scarlata & Panagia (2015), are shown with velocities relative to the 1190 Å transition. The dashed spectrum shows the pure absorption profile, whereas the solid line shows the more physically realistic model, where emission modifies absorption depths and velocities. **Right**— Real Si II spectra observed with HST appear similar to the model in the center panel. **The presence of the Si II* $\lambda\lambda 1194, 1197$ Å lines in real data implies that the absorption lines must be filled in, leading to biased outflow measurements.**

■ Analysis Plan

1. Spectral Library

The investigations described in the Science Justification requires a suite of model spectra. For this work, we will focus on the most commonly probed ions seen in HST/COS spectra: Si II, Si III, Si IV, C II, and O I, and Ly α . We will focus on 100 most massive galaxies in the SPHINX simulation ($M_* > 10^7 M_\odot$), and supplement with 11 more massive galaxies from Mitchell et al. (2018). From each simulated galaxy we will choose 10 snapshots to sample time and line-of-sight variability, post-processing the output with radiation transport to produce mock spectra in both Ly α and metal lines. These 1100 spectra will represent a benchmark that is not instrumentally affected. Then each of these will be modified to take into account the effects of various instruments. First, we will apply apertures and regenerate the spectra from the radiation transport output. We will project the 2.5" diameter COS aperture (including vignetting) to three different physical sizes, appropriate for the redshifts of the galaxies typically observed with COS. Likewise, we will apply apertures appropriate for a 0.2" slit at $z \sim 6$ (JWST/NIRSpec), and a 1" slit for $z \sim 2 - 3$. Including the “no aperture” case, we will have 6 different extractions for each time/sightline snapshot. Second, for each modeled spectrum, we will downgrade the resolution to 30, 100, and 400

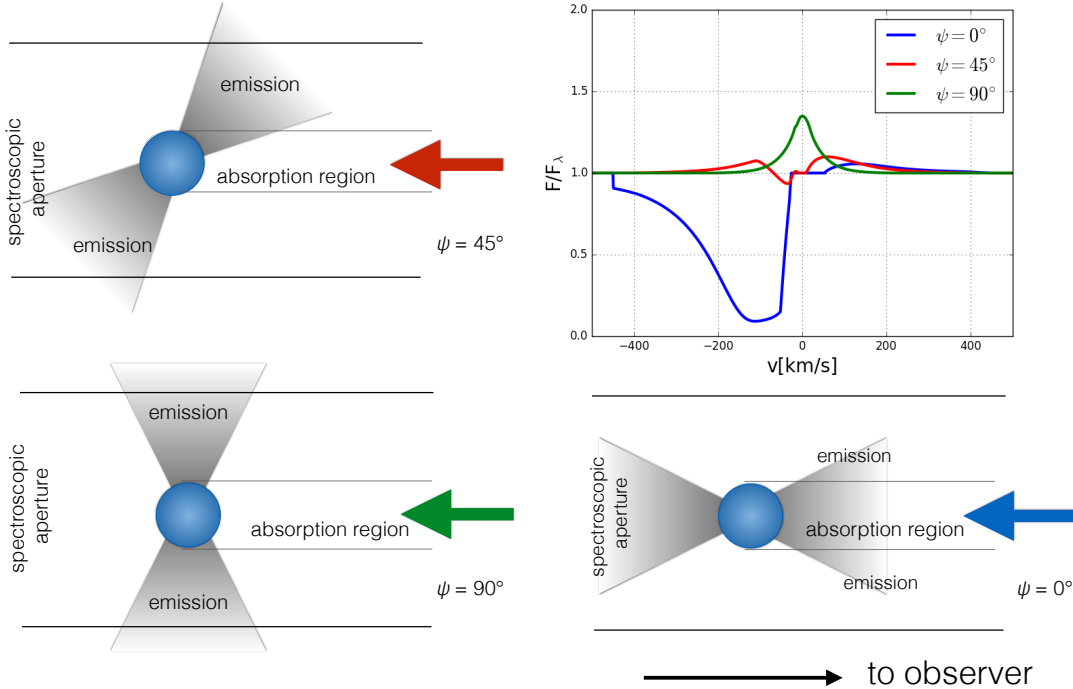


Figure 2: This cartoon sketch shows how different orientations can change the observed line profiles. The outflowing gas (grey)— a bicone arrangement in this case— both absorbs and emits photons. However, the observer can only detect absorption if the outflow occults the source, falling in the “absorption region.” Hence, the top left panel shows little absorption and some emission (red spectrum), while the lower left panel shows no absorption but significant emission (green spectrum). Similarly, the blue spectrum is almost completely in absorption; here the emission is less obvious because it extends over a broad range of observed velocities, and mostly escapes away from our line of sight.

km s⁻¹ to span the range that is (or will be) achieved with COS G140L and G130/G160M, JWST/NIRSpec, and ground-based studies (e.g. Steidel et al. 2010, Erb et al. 2012; Henry et al. 2015). Finally, we will add noise to simulate real observations. Since the simulated spectra (**Figure 3**) show some noise due to the finite number of photons propagated in the Monte Carlo radiative transfer code, we will add only the amount of noise required to bring the continuum signal-to-noise to 3, 5, 10, and 20 per resolution element. Altogether, we plan more than 79,000 spectra to sample 111 simulated galaxies.

We will draw from this library for the analyses described in the Science Justification, automating the absorption line measurements so that we can study the entire spectral library. Lastly, we note that this library of mock spectra will be released on MAST with the publication of our results. We anticipate that this artificial data will facilitate new studies, including comparison with new and existing data.

2. Relevant HST data sets

A wide number of HST/COS observations have probed outflows in metals and Ly α , sometimes finding contradictory results from the same data. Table 1 lists the COS data-sets that would benefit from having the most robust analyses, as we propose to develop. These data

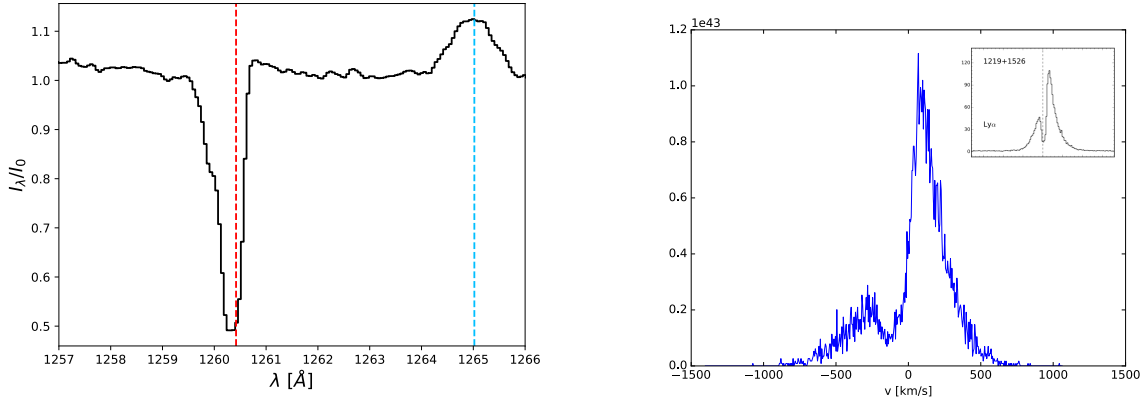


Figure 3: Post-processing of simulated galaxies with RASCAS (Michel-Dansac et al. 2019) produces realistic absorption and emission line profiles for both metal lines (left; Si II λ 1260 and Si II* λ 1265), and Ly α (right). These examples appear remarkably similar to real observations (Jaskot et al. 2014, Henry et al. 2015), as illustrated for Ly α by the inset in the right panel.

include observations in both the medium resolution gratings (G130M, G160M), and the low resolution G140L. Our mock observations will quantify how well outflows can be measured when the resolution is low. New data are being added to the archive with each observing cycle. Upon completion of our proposed studies, a re-interpretation of these data will improve constraints on outflow properties.

3. Scope of Proposed Work

The work proposed here will revolve around the analysis of mock spectra, **and will result in the publication of three papers.** The simulations are complete and radiation transport modeling is now underway (lead by un-funded, non-US co-Is). Hence, the support requested here is for “observing” the mock spectra: modeling the instrumental effects, creating the model library, making the measurements, analyzing results, writing papers, and releasing the spectral library to the public. Most of this work will be lead by a PhD student, with additional contributions from the PI and technical staff. We anticipate the following timeline:

- **Build Spectral Library:** The PhD student will create the spectral library described above, using RASCAS output provided by our Co-Is. The instrumental effects will be modeled and added. **PhD student, 2 months**
- **Measure Lines in the Spectral Library:** The PhD student will measure the emission and absorption lines in the spectral library, using automated methods. **PhD student, 2 months.**
- **Measure outflows using the conventional approach:** The PhD student will use the spectral library to measure the outflows from column densities, velocities, using standard assumptions found in the literature. These results will be compared to the simulations. **PhD student, 3 months for analysis + 3 months for writing.**

- **Measuring outflows by fitting absorption line profiles:** The PhD student will fit line profiles to the metal emission+absorption lines to measure the outflows, comparing results to the simulations. **PhD student, 3 months for analysis + 3 months for writing.**
- **Obtaining tighter constraints by including Ly α :** The PI will take the model fits from the metal lines, obtained by the PhD student, testing whether adding Ly α to the fitting procedure results in more accurate constraints on outflow properties. **PI, two months for analysis + one month for writing.**
- **Releasing the spectra to the public:** Technical staff will prepare the simulated spectra for public release on a webpage, with an easy-to-use interface. **Technical Staff, 1 month.**

Table 1. Examples of HST/COS observations sensitive to both Ly α and metal lines

Program ID	PI	Number of Galaxies	COS settings	Description
11727, 13017	Heckman	21	G130M, G160M	Lyman Break Analogs
12928	Henry	9	G130M, G160M	Green Peas
13293	Jaskot	2	G160M	Green Peas
12583	Hayes	7	G130M	Ly α Reference Sample (LARS)
13654	Hayes	27	G130M	Extended LARS (eLARS)
11522, 12027	Green	20	G130M	H α selected
13761	McCandliss	32	G140L	UV-bright galaxies
11579	Aloisi	7	G130M	Nearby Star Forming Galaxies
12173	Leitherer	4	G130M	LIRGs
14080	Jaskot	13	G130M	Green Peas
15099	Chisholm	8	G130M	Low metallicity galaxies
15340	Heckman	4	G130M	Starburst Galaxies
13744	Thuan	5	G160M, G140L	LyC Leaker Candidates
15341	Heckman	5	G140L	LyC Leaker Candidates
14571	Malkan	2	G140L	LyC Leaker Candidates
14635, 15639	Izotov	15	G160M, G140L	LyC Leaker Candidates
15626	Jaskot	67	G140L	LyC Leaker Candidates
Total		248		

Table 1: The low-redshift ($z \sim 0.02 - 0.4$) star-forming galaxies in the HST archive that will benefit from our proposed analyses. In brief, the selections are: **Lyman Break Analogs:** UV luminous, compact galaxies with properties matched to Lyman Break Galaxies at $z \sim 3$ (Heckman et al. 2011). **Green Pea Galaxies:** Extreme emission line galaxies selected from the SDSS, with high-equivalent width [O III] + H β emission dominating the r -band (Cardamone et al. 2009; Jaskot & Oey 2014; Henry et al. 2015). Some of these galaxies are also selected with size or [O III]/[O II] cuts. **LARS and eLARs:** UV and H α selected galaxies comprising the Ly α reference sample and its extension to more disk-like “normal” galaxies (Hayes et al. 2013, 2014; Rivera-Thorsen et al. 2015). **H α selected galaxies:** Prism selected galaxies from the KPNO International Spectroscopic Survey (Salzer et al. 2000; Wofford et al. 2013). **UV-bright galaxies:** A UV-bright sample targeted with lower resolution G140L spectra, selected to have high signal-to-noise at the Lyman edge. **Nearby Star Forming Galaxies** – bright point sources in nearby galaxies, with multiple sight-lines per galaxy. **LIRGs**– A complementary sample of UV bright LIRGs. **Low metallicity galaxies** – UV bright objects with low metallicities complement the more intermediate metallicity Green Peas and LBAs. **LyC leaker candidates** – galaxies selected to have potential emission of hydrogen-ionizing LyC emission. Many are confirmed LyC leakers (e.g. Izotov et al. 2016a,b, 2018a,b).

- Carr, C., et al. 2017, ApJ, 860, 143
Cardamone, C., et al. 2009, MNRAS, 399, 1191
Chevalier, R., & Clegg, A., 1985, Nature, 317, 44
Chisholm, J., et al. 2017, MNRAS, 469, 4831
Chisholm, J., et al. 2016, MNRAS, 457, 3133
Dutton, A., et al. 2012, MNRAS, 421, 608
Erb, D. K., et al. 2012, ApJ, 759, 26
Hayes, M., et al. 2013, ApJ, 765, 27L
Hayes, M., et al. 2014, ApJ, 782, 6
Heckman, T., M., et al. 2011, ApJ, 730, 5
Heckman, T. M., et al. 2015, ApJ, 809, 147
Heckman, T. M., & Borthakur, S. 2016, ApJ, 822, 9
Henry, A., et al. 2015, ApJ, 809, 19
Hopkins, P., et al. 2014, MNRAS, 445, 581
Hummels, C., B., et al. 2013, MNRAS, 430, 1548
Izotov, Y., et al. 2016a, Nature, 529, 17
Izotov, Y., et al. 2016b, MNRAS, 461, 3683
Izotov, Y., et al. 2018a, MNRAS, 474, 4514
Izotov, Y., et al. 2018b, MNRAS, 478, 4851
Jaskot, A. E., & Oey, M. S. 2014, ApJL, 791, 19
Kornei, K. A., et al. 2012, ApJ, 758, 135
Kunth, D., et al. 1998, A&A, 334, 11
Martin, C. L., et al. 2012, ApJ, 760, 127
Mitchell, P., et al. 2018, MNRAS, 474, 4279
Muratov, A. L., et al. 2015, MNRAS, 454, 2691
Oppenheimer & Davé 2008, MNRAS, 387, 577
Orlitová, I., et al. 2018, A&A, 616, 60
Prochaska, J. X., et al. 2011, ApJ, 734, 24
Rivera-Thorsen, T. E., et al. 2015, ApJ, 805, 14
Rosdahl, J., et al. 2018, MNRAS, 479, 994
Rubin, K. H. R., et al. 2014, ApJ, 794, 156
Rupke, D., et al. 2005, ApJS, 160, 115
Scarlata, C. & Panagia, N. 2015, ApJ, 801, 43
Schaye, J., et al. 2015, MNRAS, 446, 521
Steidel, C. C., et al. 2010, ApJ, 717, 289
Somerville, R., & Davé R. 2015, ARAA, 53, 51
Verhamme, A., et al. 2015, A&A, 578, 7
Vogelsberger, M., et al. 2014, MNRAS, 444, 1518
Wang, L., et al. 2015, MNRAS, 454, 83
Weiner, B. J., et al. 2009, ApJ, 692, 187
Wiener, J., et al. 2017, MNRAS, 467, 906
Wofford, A., et al. 2013, ApJ, 765, 118
Zhu, G. B., et al. 2015, ApJ, 815, 48